

Role of $4f$ states in infinite-layer NdNiO_2

Mi-Young Choi¹ and Kwan-Woo Lee^{1,2*}

¹*Department of Applied Physics, Graduate School, Korea University, Sejong 30019, Korea*

²*Division of Display and Semiconductor Physics, Korea University, Sejong 30019, Korea*

Warren E. Pickett[†]

Department of Physics, University of California, Davis, California 95616, USA

(Dated: November 29, 2021)

Atomic $4f$ states have been found to be essential players in the physical behavior of lanthanide compounds, at the Fermi level E_F as in the proposed topological Kondo insulator SmB_6 , or further away as in the magnetic superconductor system $\mathcal{R}\text{Ni}_2\text{B}_2\text{C}$ (\mathcal{R} =rare earth ion) and in $\text{Y}_{1-x}\text{Pr}_x\text{Ba}_2\text{Cu}_3\text{O}_7$, where the $4f$ shell of Pr has a devastating effect on superconductivity. In hole-doped $\mathcal{R}\text{NiO}_2$, the \mathcal{R} =Nd member is found to be superconducting while \mathcal{R} =La is not, in spite of the calculated electronic structures being nearly identical. We report first principles results that indicate that the Nd $4f$ moment affects states at E_F in infinite-layer NdNiO_2 , an effect that will not occur for LaNiO_2 . Treating 20% hole-doping in the virtual crystal approach indicates that 0.15 holes empty the Γ -centered Nd-derived electron pocket while leaving the other electron pocket unchanged; hence Ni only absorbs 0.05 holes; the La counterpart would behave similarly. However, coupling of $4f$ states to the electron pockets at E_F arises through the Nd intra-atomic $4f - 5d$ exchange coupling $K \approx 0.5$ eV and is ferromagnetic (FM), *i.e.* anti-Kondo, in sign. This interaction causes spin-disorder broadening of the electron pockets and should be included in models of the normal and superconducting states of $\text{Nd}_{0.8}\text{Sr}_{0.2}\text{NiO}_2$. The Ni moments differ by $0.2\mu_B$ for FM and antiferromagnetic alignment (the latter are larger), reflecting some itineracy and indicating that Heisenberg coupling of the moments may not provide a quantitative modeling of Ni-Ni exchange coupling.

I. BACKGROUND AND MAJOR ISSUES

The discovery of superconductivity up to $T_c=15$ K in Sr-doped NdNiO_2 ($\text{Nd}_{0.8}\text{Sr}_{0.2}\text{NiO}_2$)[1] has re-invigorated the three decade long issue of whether there may be nickelates that can host cuprate-type superconductivity. LaNiO_2 , which is isostructural with “infinite layer” CaCuO_2 [2] that superconducts up to 110 K when doped,[3] has been one of the prime candidates, but what doping is possible has never resulted in superconductivity. NdNiO_2 is also isovalent with CaCuO_2 , providing a nominal d^9 configuration on the open shell transition metal ion.

Early comparison of the electronic structures of CaCuO_2 and NdNiO_2 identified similarities but substantial differences,[4, 5] with questions about whether concepts such as strong superexchange coupling of the transition metal moments, or of Zhang-Rice singlets upon doping,[1] are relevant to this nickelate. A number of groups recently have revisited this question, with the objective of few-band model-building to quantify differences related to superconductivity.[6–19] The popular approach has been to obtain the non-magnetic local density approximation (LDA) band structure of NdNiO_2 with the $4f^3$ electrons assigned to a non-magnetic core, then approximate the low energy bands with a minimal local orbital model, add a repulsive local interaction, and

evaluate the consequences, *viz.* the pairing susceptibility. Close attention is given to the geometry of the Fermi surface (FS), which strongly impacts the pairing susceptibility.

Detailed analyses of the LDA electronic structure have been provided by Botana and Norman[6] for LaNiO_2 and by Nomura *et al.*[9] for NdNiO_2 , in which three non-magnetic $4f$ electrons are included in the Nd core. In addition to the roughly half-filled Ni $3d_{x^2-y^2}$ band, several groups find and quantify Nd $5d$ derived bands obtained earlier.[4, 5] A Nd $5d_{z^2}$ band drops below the Fermi level E_F at Γ , and in addition a band usually identified as Nd $5d_{xy}$ -derived drops below E_F at the zone corner $A=(\pi, \pi, \pi)$ point [in units of $(\frac{1}{a}, \frac{1}{a}, \frac{1}{c})$]. This undoped NdNiO_2 FS differs in significant ways from that of nonmagnetic CaCuO_2 but is similar to LaNiO_2 . X-ray absorption spectra of the O K and Ni L_3 edges[20] do not reveal significant differences between LaNiO_2 and NdNiO_2 .

There are other fundamental questions to be considered. Experimentally, undoped CaCuO_2 orders antiferromagnetically with a high Neel temperature of 442 K,[21] while undoped NdNiO_2 and LaNiO_2 do not order.[1] The underlying differences with cuprates are several. The mean Ni $3d$ level ϵ_d is separated from the O $2p$ level ϵ_p by 4 eV in the nickelates versus only 2 eV in the cuprate.[6] Ni therefore has less hybridization with oxygen $2p$ orbitals than does Cu, thus should have a stronger tendency toward local moment magnetism than does Cu, and indeed it does so in LDA calculations. The superexchange coupling J is much smaller for the nickelate,[6] thus one expects a lower but nonzero Neel temperature.

*Electronic address: mckwan@korea.ac.kr

†Electronic address: wepickett@ucdavis.edu

Finally, LaNiO_2 and NdNiO_2 are reported as conducting (albeit poorly), whereas CaCuO_2 is insulating. Lack of Ni ordering is a central question to address; however, both in calculations and experimentally the nickelates are conducting. We note that magnetic order disappears in cuprates when they are doped to become conducting.

The model treatments mentioned above would suggest that doped LaNiO_2 should be superconducting as is doped NdNiO_2 . Since this is not the case, we pursue the viewpoint that a more fundamental question is what features may account for this difference between two highly similar nickelates. La and Nd are very similar chemically, with tri-positive ionic radii only slightly larger for La than for Nd. Although small size differences in lattice constants or strains can influence states in correlated insulators, itineracy and screening by carriers strongly reduce such effects.

An obvious difference between these nickelates is that La^{3+} is closed shell and nonmagnetic, whereas Nd^{3+} , with Hund's rule ground state $S = \frac{3}{2}, L = 6, J = \frac{9}{2}$, has a (free ion) Curie-Weiss moment of nearly $4 \mu_B$. Superconductivity appears in $\text{Nd}_{0.8}\text{Sr}_{0.2}\text{NiO}_2$ in the midst of these large disordered local moments, which should compete with superconducting phases, directly or by introducing disorder into the electronic structure. In several YBCO-type cuprates, however, replacing a nonmagnetic rare earth ion (La or Y) by a magnetic lanthanide from Dy to Tb does not affect the superconductivity, because the small $4f$ orbital is not involved in the electronic structure. Surprisingly, $\text{PrBa}_2\text{Cu}_3\text{O}_7$ was found to be non-superconducting,[22] due to antibonding coupling of the Pr $4f_{z(x^2-y^2)}$ orbital to the O $2p$ orbitals.[23, 24] Notably, the local environment of the $4f$ ion is the same as in NdNiO_2 .

Another related system is the rare earth nickel borocarbides $\mathcal{R}\text{Ni}_2\text{B}_2\text{C}$ where \mathcal{R} can be one of many of the rare earth atoms. This system displays strong interplay and competition between the \mathcal{R} $4f$ magnetic moment and the conduction states with heavy Ni character, with the \mathcal{R} $5d$ playing an important role in coupling the local moments to the itinerant states.[25, 26] Elemental europium at high pressure but retaining a f^7 local moment, switches from metallic and magnetically ordered to superconducting and magnetically disordered around 80 GPa,[27, 28] providing its own questions about the effect of $4f$ moments on pairing, a coupling that must proceed through the Eu $5d$ states.

The question of possible impact of the $4f$ shell has not been addressed in NdNiO_2 . While direct $4f$ -nickelate hybridization may be small, there is an intra-atomic exchange coupling between the $4f$ spin and the $5d$ states around E_F that, as mentioned, does not occur in LaNiO_2 . Since the $5d$ bands cross E_F , carriers will be affected. Specifically, with disordered Nd moments, the $5d$ on-site energies will be spin-split, with a projection along any given direction that is distributed randomly. A carrier in a $5d$ band will be subjected to a random potential, resulting in band broadening and magnetic scattering that

is absent in LaNiO_2 .

The presentation is organized as follows. The computational methods and material configurations are described in Sec. II. In Sec. III results are presented for four assumed types of magnetic order in NdNiO_2 . The electronic bands and Fermi surfaces for non-magnetic Ni are discussed in Sec. IV. A few results relating to the occupied Nd $4f$ orbitals are presented in Sec. V, followed by a discussion of hole doping in Sec. VI. Some observations about the effects of magnetic order and relation to other $4f$ -containing superconductors are made in Sec. VII, which is followed by a brief summary in Sec. VIII.

II. COMPUTATIONAL METHODS

We have studied the electronic and magnetic properties of NdNiO_2 using the precise, all-electron, full potential linearized augmented planewave method as implemented in WIEN2K[29]. The lattice constants $a = 3.92 \text{ \AA}$, $c = 3.37 \text{ \AA}$ observed for superconducting $\text{Nd}_{0.8}\text{Sr}_{0.2}\text{NiO}_2$ [1] have been used, all atoms lie at $P4/mmm$ symmetry determined positions. Strong intra-atomic interactions on Nd, and usually on Ni in nickelates, are modeled with the DFT+U method[30] (density functional theory plus Hubbard U), which is essential to preserve the $4f$ local moment and place the corresponding bands away from E_F . The fully anisotropic, rotationally invariant DFT+U correlation correction functional in the fully localized limit form[31] implemented in WIEN2K, was used. Results are presented for $U_f^{Nd}=8.0 \text{ eV}$, $J_f^{Nd}=1.0 \text{ eV}$, $U_d^{Ni}=5.0 \text{ eV}$, and $J_d^{Ni}=0.7 \text{ eV}$ (and occasionally for $U_d^{Ni}=0$). Other input parameters and a survey of results beyond those presented here are provided in the Supplemental Material (SM).[32] Section VI was carried out by reducing the nuclear charge on Nd by 0.20, and removing the same amount of electrons.

The strong local $4f$ moment requires magnetically ordered calculations. We find that Ni prefers a moment of the order of $0.5 \mu_B$ without any U^{Ni} , which increases to $\sim 1 \mu_B$ for the values we have used. The Nd moment always assumes the spin value of $3 \mu_B$ characteristic of an f^3 Hund's rule ion, plus minor exchange polarization of the $5d$ orbitals. We have studied four magnetic configurations:

AFM0: antiferromagnetic (AFM) Nd layers with non-magnetic Ni layers;

AFM1: both Ni and Nd layers have antialigned moments; AFM2: ferromagnetic (FM) Nd layers and AFM Ni layers; and

FM: all Nd and Ni moments aligned.

Note that it is the AFM1 and AFM2 cases in which Ni is antiferromagnetically ordered. Note also that AFM0 is done with $U_d^{Ni}=0$, so its energy cannot be compared with the other cases.

The SM provides additional information about the electronic structures. An insulating band structure is never obtained, which is a great difference compared with

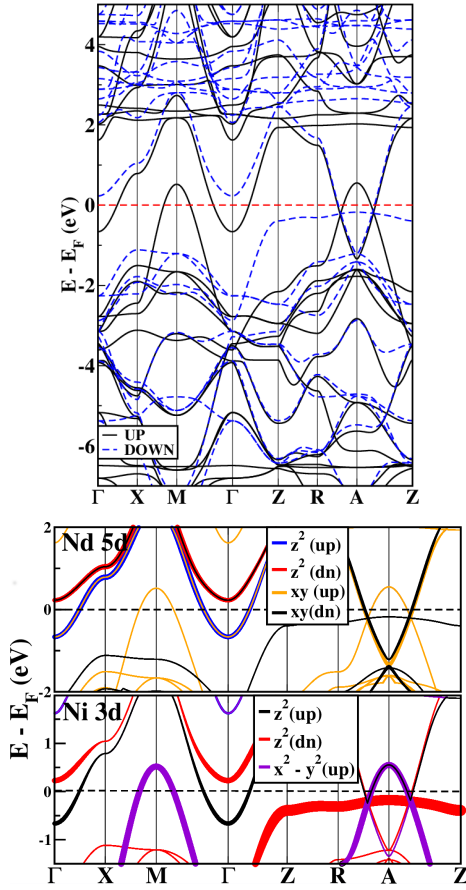


FIG. 1: Top: GGA+U FM bands of NdNiO₂: solid lines denote majority, dashed lines indicate minority, and E_F is the zero of energy. Bottom: Color fatband plot of FM NdNiO₂ near E_F , with the legend describing the color choice. Note the Nd-derived electron pockets at Γ and A , and the Ni majority $d_{x^2-y^2}$ hole pockets at M and A .

cuprates. It was shown earlier that increasing U on Ni in NdNiO₂ never leads to a Mott insulator, instead a $3d_{z^2}$ orbital becomes unoccupied and forms a peculiar intra-atomic singlet with the $d_{x^2-y^2}$ orbital.[5]

III. MAGNETIC ORDER

Although it is expected that Ni¹⁺ d^9 ions will tend to order in antiferromagnetic (AFM1 or AFM2) fashion through superexchange as does CaCuO₂ and several other d^9 cuprates, we begin with FM alignment within both Ni and Nd layers, as it enables identification of the intra-atomic exchange splitting between the occupied Nd $4f$ and conduction $5d_{z^2}$ orbitals.

A magnetic Ni ion leads to a 120 meV energy gain compared to non-magnetic. This exaggerated tendency toward magnetic ordering and the magnitude of the magnetic moment are a known deficiency of (semi)local density functional methods, with much of the problem attributed to the lack of effects of spin fluctuations in the

functional.

The energies can be compared for those cases with magnetic Ni (AFM1, AFM2, FM) for which the same functional is used. The energy of AFM2 (FM Nd) is slightly lower than that of AFM1 (AFM Nd), by 7 meV for $U^{Ni}=0$ and by only 1 meV (at the edge of computational precision) with $U^{Ni}=5$ eV, reflecting a slight tendency toward FM ordering of the $4f$ moments. The energy difference between FM and AFM2 provides the difference between AFM and FM Ni moment alignment; AFM is favored by 116 (25) meV/Ni in GGA(+U). This energy difference contains information about Ni-Ni in-plane exchange coupling, and would give a value of the nearest neighbor coupling if more distant exchange couplings were negligible. Liu *et al.* have derived values of coupling for a few neighbors, concluding that the values depend strongly on the value of U^{Ni} that is assumed.[18]

For the FM bands shown in Fig. 1 the Ni and Nd moments are aligned into an overall FM structure. The Ni $d_{x^2-y^2}$ bands that give rise to the large FS are spin-split by 2 eV, reflecting the Ni spin moment of order $1\mu_B$. As noted earlier[4, 5] and recently by several others, Nd $5d$ -derived bands dip below E_F at the zone center Γ and at the zone corner A , with bonding $5d_{z^2}$ and antibonding $5d_{xy}$ character respectively.[9] There is mixing with Ni d_{z^2} in both of these electron pockets, especially the latter. This mixing is due to the surprise that the minority (but occupied) Ni d_{z^2} antibonding band at $k_z = \pi$ (see the $Z - R - A - Z$ lines) lies within 0.2–0.4 eV of E_F .

As shown in Fig. 1, the $5d_{z^2}$ band energies relative to E_F of up (down) bands are -0.7 ($+0.3$) eV at Γ , giving an intra-atomic coupling $H^{Nd} = K\hat{e}_{4f} \cdot \hat{e}_{5d}$ with $K=0.5$ eV, in terms of the orientations of the $4f$ and $5d$ spins. For the antibonding $5d_{xy}$ orbital the eigenvalues at A lie at -1.2 eV with a splitting of less than 0.1 eV, reflecting the participation of Ni $3d$ orbitals and the out-of-phase character of states at the A point. Note that this coupling is Hund's rule alignment of $4f$ and $5d$ states and therefore anti-Kondo coupling of the local moment to the conduction band, as opposed to some suggested Kondo modeling of Nd_{0.8}Sr_{0.2}NiO₂. [4, 20] Such anti-Kondo coupling has been studied in other lanthanide compounds.[33] We return below to the $K \approx 0.5$ eV intra-atomic exchange coupling of Nd $5d$ states.

IV. NONMAGNETIC Ni AND FERMI SURFACES

Low energy models of oxides including superconducting possibilities are based on non-magnetic Ni, with an on-site repulsion added to provide correlated electron behavior and a potential pairing mechanism. We have obtained a DFT+U solution with non-magnetic Ni ($U_d^{Ni}=0$, $U_f^{Nd}=8$ eV), our case AFM0. The Nd $4f$ moment that must remain fully spin-polarized has AFM alignment, so the Brillouin zone is correspondingly folded back. The Ni moment for AFM alignment is $1.2\mu_B$, compared to $1.0\mu_B$

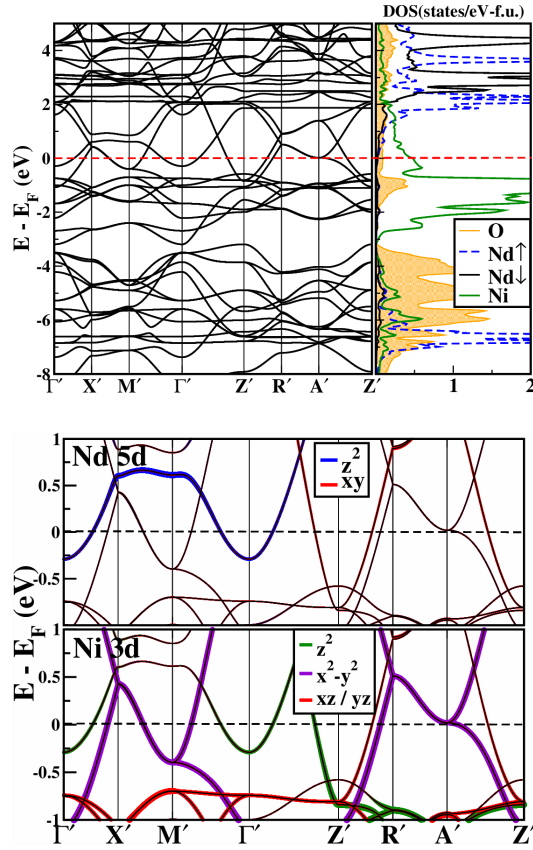


FIG. 2: Top: Bands of NdNiO₂, with AFM Nd moments and non-magnetic Ni layer, plotted along lines in the AFM zone. Bottom: Fatbands indicating Nd 5d character (above) and Ni 3d weight (below), with orbital character as noted. In terms of the usual NiO₂ sublattice, the $M(A)$ point is folded back to $\Gamma'(Z')$. The other symmetry points are $X' = (\pi/2, \pi/2, 0)$ and $M' = (\pi, 0, 0)$, while R' and A' lie above these points by $(0, 0, \pi)$ respectively.

for FM alignment. For $U=0$ (just GGA) the calculated moments are $0.52\mu_B$ (AFM) and $0.35\mu_B$ (FM); *i.e.* there is about $0.2\mu_B$ difference in the moments, and the associated Hund's energy would be an important contribution to the lower energies for AFM alignment.

The bands, density of states (DOS), and fatbands near E_F for AFM0 alignment are shown in Fig. 2, with symmetry points in that folded tetragonal zone now designated with primes. Gaps at the zone boundaries indicate effects of the Nd AFM order, *e.g.* a gap of 0.3 eV can be seen in the Nd 5d band around 0.8 eV at X' . As for the FM order above, this splitting vanishes for the corresponding antibonding band at R' . The nearby folded Ni 3d band displays no gap, reflecting canceling mixing with the eight neighboring Nd sites.

The bands crossing E_F giving the FSs are those that are fit to few band models. The corresponding FSs are shown in Fig. 3. The Nd $5d_{z^2}$ related electron pocket Pk1 at Γ has attracted attention, with the electron pocket Pk2 at $A=(\pi, \pi, \pi)$ [Z' in Fig. 2] also receiving notice.

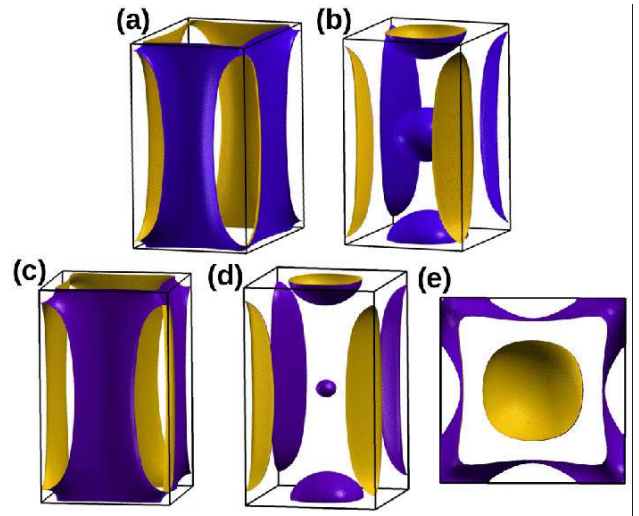


FIG. 3: Fermi surfaces for case AFM0 (non-magnetic Ni), in the full zone corresponding to AFM $4f$ alignment. Surfaces have been separated into left and right sub-panels for clarity. (a),(b) Undoped NdNiO₂. The spheres are (i) the Nd $5d$ electron pocket at $\Gamma' = \Gamma$, at the center of the figure, and (ii) the other electron pocket at A folded back to Z' (see text). (c),(d): Surfaces for VCA Nd_{0.8}Sr_{0.2}NiO₂, $x=0.20$ hole doping. The Γ -centered electron pocket is essentially emptied, while the Z' -centered pocket is almost unchanged. (e) Top view of the Nd_{0.8}Sr_{0.2}NiO₂ surfaces, showing the amount of k_z dispersion.

Pk2 has strong Ni $3d_{z^2}$ character as well as some $3d_{xz,yz}$ influence, considerably stronger than the Nd $5d_{xy}$ component that has been discussed by several groups.[5–10] Due to k_z dispersion, the large Ni $d_{x^2-y^2}$ FS appears in this folded zone as a large banana centered at M' , and strongly fluted cylinders also centered at M' and connected by tiny necks at the corner R' points. These two surfaces are degenerate along the zone faces reflecting simple folding back into the AFM zone, and correspond to M -centered hole barrels in the primitive zone that are familiar from cuprate physics. These barrels have surprisingly large k_z dispersion, lessening the relevance of two dimensional physics.

V. OCCUPIED $4f$ ORBITALS

We now consider briefly the Nd $4f$ contributions to the electronic and magnetic structure. The $S = \frac{3}{2}$ spin configuration is strongly enforced by Hund's first rule, and the energy difference between FM and AFM order of the Nd moments is very small; ~ 7 meV/Nd ion for Ni treated in GGA, and only 1 meV/Nd ion for Ni treated in GGA+U. The three occupied bands lie at -7 eV with some small dispersion due to the direct overlap of $4f$ and O $2p$ orbitals, which is small but provides crystal field splitting of the $4f$ orbitals. The occupied states that we obtained are combinations of $m_\ell = -3, -2, +1$,

each with lesser admixtures of $+1, +2, -3$ states, respectively, with total orbital moment $m_{orb}=4.47 \mu_B$. When spin-orbit coupling is included, the occupied orbitals are those with $j = \frac{5}{2}, m_j = -\frac{5}{2}, -\frac{3}{2}, +\frac{1}{2}$. (See SM for further information on these occupations.) The four unoccupied $4f$ bands are centered 3.5 eV above E_F but are spread by the anisotropy of the orbitals and mixing with Nd $5d$ states over a range of 3 eV.

VI. HOLE DOPING

NdNiO₂ becomes superconducting upon hole doping by 0.2 hole/f.u.[1] With the Fermi level density of states $N(0)=0.70/(\text{eV cell})$, the drop in E_F (in rigid band) is 0.29 eV, which is enough to empty the Pk1 pocket at Γ to 0.4 eV, and to reduce the carrier density of Pk2 but leaving substantial Ni carriers. Rigid band treatment may be deceptive, however, due to Fermi level charge on both Ni and Nd atoms. We applied the virtual crystal approximation[34] (VCA) to obtain a more realistic effect of doping.

Fermi surfaces Pk1 and Pk2 of undoped [Figs. 3(a) and 3b)] and $x=0.20$ doped NdNiO₂ [Figs. 3(c)-3(e)] reveal important non-rigid band behavior, and the corresponding bands provided in Fig. 4 indicate the reason. The Ni d bands are shifted only slightly (~ 0.1 eV) with respect to E_F by doping, as is the band giving the A-centered pocket (at Z' in this figure). The Nd $5d$ band at Γ is, however, shifted by 0.3 eV and effectively emptied of its (undoped) 0.15 electrons. These VCA bands are similar to the VCA bands of Sakakibara *et al.*[7] for La_{0.8}Ba_{0.2}NiO₂, a difference being that their La $5d$ band is 0.2 eV higher than our Nd $5d$ band.

The band giving rise to Pk2, often referred to as Nd $5d_{xy}$, is also heavily Ni in character (shown above, and in the SM), hence little affected as are the other Ni $3d$ bands. The result is that $x = 0.20$ doping changes the Ni $3d$ charge by only 0.05 holes. The disappearance of pocket Pk1 and its associated disorder scattering may contribute to the drop in resistivity by a factor of 2–3 upon doping.[1]

VII. IMPLICATION OF SPIN DISORDER

The exchange splitting of the Nd $5d$ band at Γ (near E_F) reflects the intra-atomic $4f - 5d$ exchange on Nd of $K \approx 0.5$ eV. The $S = \frac{3}{2}$ spin moment on Nd drives this exchange splitting, which will follow the orientation of the $4f$ moment, which is disordered. With the very weak $4f - 4f$ exchange coupling noted in Sec. III, the Nd moments will be randomly oriented and quasi-static on an electronic time scale.

In spite of the disorder broadening on the electron Fermi pockets and resulting strong spin scattering driven by stable, essentially classical but disordered $4f$ moments, superconductivity survives in Nd_{0.8}Sr_{0.2}NiO₂.

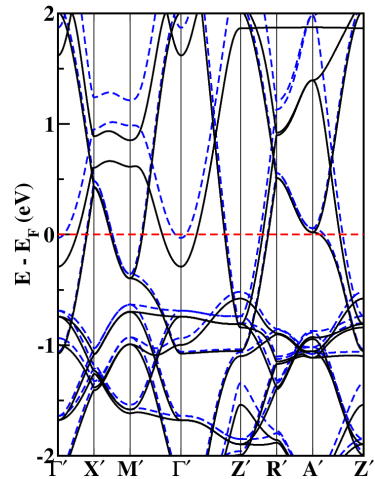


FIG. 4: Band structures of Nd_{0.8}Sr_{0.2}NiO₂ (dashed lines) compared to those of NdNiO₂ (solid lines), near E_F . Here $U_d^{Ni} = 0$; Ni is non-magnetic. The bands are plotted in the Nd AFM zone. Note that hole doping removes electrons primarily from the Γ -centered Nd $5f$ electron pocket; the Z' (A in primitive zone) pocket is nearly unchanged.

This situation bears some similarity to that of elemental Eu with its $4f^7$ moment: pressure kills magnetic order around 82 GPa but not the local moment, and there is a first order electronic but isostructural transformation to a superconducting phase at 1.7 K.[27] The exchange coupling from the classical local moment that should be disruptive to Cooper pairing in a specific spin configuration (singlet or triplet) may actually be contributing to the pairing in Eu.[28] The exchange coupling in NdNiO₂ is not as pervasive – every site in Eu has a $4f$ moment and the partially occupied conduction band is entirely $5d$ – but some of the physics may be related.

A related, and commonly modeled, spin-scattering process will occur on the (locally) magnetic Ni ion (as treated for the Cu ion in cuprates), an effect that can be modeled by any of a variety of spin fluctuation formalisms applicable to transition metal oxides. The resulting strong scattering in the electron pockets is a potential contributor to the resistivity of “conducting” NdNiO₂, where the resistivity $\rho \sim 1 m\Omega\text{cm}$ varies little between 300 K and the lowest temperature measured. The inferred mean free path in a Fermi liquid inspired Bloch-Boltzmann treatment would be atomic size, meaning incoherent transport and a washed out FS. A dynamical mean field approximation treatment of Ni $3d$ fluctuations[11] in LaNiO₂ found little shifting and broadening of bands around E_F , and no mechanism for the high resistivity. The large residual resistivity may be the result of the topotactic synthesis technique, with indications to be learned between the similarities and the distinctions between the doped thin films and doped bulk materials,[35] which also have similarly high residual resistivity.

VIII. SUMMARY

In this work we have focused on a primary distinction between NdNiO_2 and LaNiO_2 . When the $4f$ moment on Nd is relegated to the core in nonmagnetic fashion, the electronic structures are nearly identical. Yet the Nd compound becomes superconducting while the sister La compound remains non-superconducting, when 20% hole-doped. We find that the strong Nd $4f$ moment is intra-atomic exchange-coupled to the Nd $5d$ orbitals by a coupling of roughly $K=0.5$ eV, giving anti-Kondo coupling between the Nd local moments and the lower conduction band. The disordered $4f$ moments will give rise to a broadening of $5d$ bands of the order of K , affecting transport and perhaps becoming implicated in pairing, either as a participant or a disruptive agent.

The calculated Ni moments are larger by $0.2\mu_B$ for antiferromagnetic alignment than for ferromagnetic alignment. The associated Hund's rule energy provides a tendency toward AFM alignment that lies beyond the usual Heisenberg exchange coupling picture. An important feature of this system is that the Γ -centered Nd $5d$ Fermi surface pocket accepts most of the doped holes, leaving

Ni $3d$ charge changed only by 0.05 holes for 20% doping. The Pk2 spherical Fermi surface pocket that remains intact after doping, and rather strong k_z fluting of the Ni Fermi surfaces, suggests the importance of k_z dispersion (three dimensionality). Our results indicate that several aspects of the Nd ion arising from the open $4f$ shell require attention for understanding both normal and superconducting state properties.

Note Added: A useful reference has just appeared on the APS Condensed Matter Physics Journal Club postings. [36].

IX. ACKNOWLEDGMENTS

We acknowledge informative discussions with A. S. Botana, J. Sun, M. J. Han, E.-G. Moon, D. Lee, and J. Son, and communication with S. Raghu. M.Y.C. and K.W.L were supported by National Research Foundation of Korea Grants No. NRF-2019R1A2C1009588. W.E.P. was supported by NSF Grant No. DMR 1607139.

-
- [1] D. Li, K. Lee, B. Y. Wang, M. Osada, S. Crossley, H. R. Lee, Y. Cui, Y. Hikita, and H. Y. Hwang, Superconductivity in an infinite-layer nickelate, *Nature* **572**, 624 (2019).
 - [2] T. Siegrist, S. M. Zahurak, D. W. Murphy, and R. S. Roth, The parent structure of the layered high-temperature superconductors, *Nature* **334**, 231 (1988).
 - [3] M. Azuma, Z. Hiroi, M. Takano, Y. Bando, and Y. Takeda, Superconductivity at 110 K in the infinite-layer compound $(\text{Sr}_{1-x}\text{Ca}_x)_{1-y}\text{CuO}_2$, *Nature* **356**, 775 (1992).
 - [4] V. I. Anisimov, D. Bukhvalov, and T. M. Rice, Electronic structure of possible nickelate analogs to the cuprates, *Phys. Rev. B* **59**, 7901 (1999).
 - [5] K.-W. Lee and W. E. Pickett, Infinite Layer LaNiO_2 : Ni^{1+} is not Cu^{2+} , *Phys. Rev. B* **70**, 165109 (2004).
 - [6] A. S. Botana and M. R. Norman, Similarities and differences between infinite-layer nickelates and cuprates and implications for superconductivity, arXiv:1908.10946.
 - [7] H. Sakakibara, H. Usui, K. Suzuki, T. Kotani, H. Aoki, and K. Kuroki, Model construction and a possibility of cuprate-like pairing in a new d^9 nickelate superconductor $(\text{Nd,Sr})\text{NiO}_2$, arXiv:1909.00060.
 - [8] X. Wu, D. D. Sante, T. Schwemmer, W. Hanke, H. Y. Hwang, S. Raghu, and R. Thomale, Robust $d_{x^2-y^2}$ -wave superconductivity of infinite-layer nickelates, arXiv:1909.03015.
 - [9] Y. Nomura, M. Hirayama, T. Tadano, Y. Yoshimoto, K. Nakamura, and R. Arita, Formation of 2D single-component correlated electron system and band engineering in the nickelate superconductor NdNiO_2 , *Phys. Rev. B* **100**, 205138 (2019).
 - [10] J. Gao, Z. Wang, C. Fang, and H. Weng, Electronic Structures and Topological Properties in Nickelates $\text{Ln}_{n+1}\text{Ni}_n\text{O}_{2n+2}$, arXiv:1909.04657.
 - [11] S. Ryee, H. Yoon, T. J. Kim, M. Y. Jeong, and M. J. Han, Induced Magnetic Two-dimensionality by Hole Doping in Superconducting $\text{Nd}_{1-x}\text{Sr}_x\text{NiO}_2$, arXiv:1909.05824.
 - [12] G.-M. Zhang, Y.-F. Yang, and F.-C. Zhang, Self-doped Mott insulator for parent compounds of nickelate superconductors, arXiv:1909.11845.
 - [13] H. Zhang, L. Jin, S. Wang, B. Xi, X. Shi, F. Ye, and J.-W. Mei, Effective Hamiltonian for superconducting Ni oxides $\text{Nd}_{1-x}\text{Sr}_x\text{NiO}_2$, arXiv:1909.07427.
 - [14] Y.-H. Zhang and A. Vishwanath, Kondo resonance and d-wave superconductivity in the t-J model with spin one holes: possible applications to the nickelate superconductor $\text{Nd}_{1-x}\text{Sr}_x\text{NiO}_2$, arXiv:1909.12865.
 - [15] P. Jiang, L. Si, Z. Liao, and Z. Zhong, Electronic structure of rare-earth infinite-layer ReNiO_2 ($\text{Re}=\text{La}, \text{Nd}$), *Phys. Rev. B* **100**, 201106(R) (2019).
 - [16] L.-H. Hu and C. Wu, Two-band model for magnetism and superconductivity in nickelates, *Phys. Rev. Research* **1**, 032046(R) (2019).
 - [17] P. Werner and S. Hoshino, Nickelate superconductors: multiorbital nature and spin freezing, arXiv:1910.00473.
 - [18] Z. Liu, Z. Ren, W. Zhu, Z. F. Wang, and J. Yang, Electronic and magnetic structure of infinite-layer NdNiO_2 : trace of antiferromagnetic metal, arXiv:1912.01332.
 - [19] M. Jiang, M. Berciu, and G. A. Sawatzky, Doped holes in NdNiO_2 and high- T_c cuprates show little similarity, arXiv:1909.02557.
 - [20] M. Hepting, D. Li, C. J. Jia, H. Lu, E. Paris, Y. Tseng, X. Feng, M. Osada, E. Been, Y. Hikita, Y.-D. Chuang, Z. Hussain, K. J. Zhou, A. Nag, M. Garcia-Fernandez, M. Rossi, H. Y. Huang, D. J. Huang, Z. X. Shen, T. Schmitt, H. Y. Hwang, B. Moritz, J. Zaanen, T. P. Devereaux, and W. S. Lee, Electronic structure of the parent compound of superconducting infinite-layer nickelates,

arXiv:1909.02678.

- [21] K. Mikhalev, S. Verkhovskii, A. Gerashenko, A. Mirmelstein, V. Bobrovskii, K. Kumagai, Y. Furukawa, T. D'yachkova, and Yu. Zainulin, Temperature dependence of the sublattice magnetization of the infinite-layer antiferromagnet SrCuO_2 , *Phys. Rev. B* **69**, 132415 (2004).
- [22] H. B. Radousky, A review of the superconducting and normal state properties of $\text{Y}_{1-x}\text{Pr}_x\text{Ba}_2\text{Cu}_3\text{O}_7$, *J. Mater. Res.* **7**, 1917 (1992).
- [23] A. I. Liechtenstein and I. I. Mazin, Quantitative Model for the Superconducting Suppression in $\text{R}_{1-x}\text{Pr}_x\text{Ba}_2\text{Cu}_3\text{O}_7$ with Different Rare earths, *Phys. Rev. Lett.* **74**, 1000 (1995).
- [24] W. E. Pickett and I. I. Mazin, $\text{RBa}_2\text{Cu}_3\text{O}_7$ Compounds: Electronic Theory and Physical Properties, *Handbook on the Physics and Chemistry of Rare Earths*, edited by K. A. Gschneidner, Jr., L. Eyring, and M. B. Maple (Elsevier, Amsterdam, 2000), pp. 453-489.
- [25] L. C. Gupta, Superconductivity and magnetism and their interplay in quaternary borocarbides $\text{RNi}_2\text{B}_2\text{C}$, *Adv. in Phys.* **55**, 691 (2006).
- [26] W. E. Pickett and D. J. Singh, New Class of Intermetallic Borocarbides: Electron-Phonon Coupling and Physical Parameters, *J. Supercond.* **8**, 425 (1995).
- [27] M. Debessai, T. Matsuoka, J. J. Hamlin, J. S. Schilling, and K. Shimizu, Pressure-induced superconducting state of europium metal at low temperatures, *Phys. Rev. Lett.* **102**, 197002 (2009).
- [28] S.-T. Pi, S. Y. Savrasov, and W. E. Pickett, Pressure-tuned Frustration of Magnetic Coupling in Elemental Europium, *Phys. Rev. Lett.* **122**, 057201 (2019).
- [29] K. Schwarz and P. Blaha, Solid state calculations using WIEN2k, *Comput. Mater. Sci.* **28**, 259 (2003).
- [30] E. R. Ylvisaker, K. Koepernik, and W. E. Pickett, Anisotropy and magnetism in the LSDA+U method, *Phys. Rev. B* **79**, 035103 (2009).
- [31] A. B. Shick, A. I. Liechtenstein, and W. E. Pickett, Implementation of the LDA+U Method Using the Full Potential Linearized Augmented Plane Wave Basis, *Phys. Rev. B* **60**, 10763 (1999).
- [32] See Supplemental Material at [URL provided by the publisher] where information is provided on the DFT method and several results beyond those in the manuscript..
- [33] J. Kuneš and W. E. Pickett, Kondo and anti-Kondo coupling to local moments in EuB_6 , *Phys. Rev. B* **69**, 165111 (2004).
- [34] The VCA was accomplished by replacing $Z=60$ of Nd by $Z=59.8$. The small shift in $4f$ levels is unimportant.
- [35] Q. Li, C. He, J. Si, X. Zhu, Y. Zhang, and H.-H. Wen, Absence of superconductivity in bulk $\text{Nd}_{1-x}\text{Sr}_x\text{NiO}_2$, arXiv:1911.02420.
- [36] A. Fujimori, Electronic structure, magnetism, and superconductivity in infinite-layer nickelates, *Journal Club for Condensed Matter Physics*, December (2019).

X. SUPPLEMENTAL MATERIAL

Calculation Methods

Our calculations with WIEN2K were based on the generalized gradient approximation (GGA)[1]. The effects of correlation were treated with the GGA+U approach in the fully localized limit. In the GGA+U calculations presented here, we focused on the results of the Hubbard $U = 8(5)$ eV and Hund's coupling $J = 1(0.7)$ eV for the Nd $4f$ (Ni $3d$), except where noted. Our conclusions weren't affected by varying the value of U by 1–2 eV.

In WIEN2K, the basis size was determined by $R_{mt}K_{max} = 8$; checking $R_{mt}K_{max}=9$ gave no noticeable difference. The APW radii were chosen as Nd 2.50, Ni 1.98, and O 1.70, in atomic units. Convergence was checked with dense k -meshes up to $29 \times 29 \times 34$ to treat the highly localized $4f$ orbitals carefully.

Fermi surface of $\text{Nd}_{0.8}\text{Sr}_{0.2}\text{NiO}_2$ in rigid band approximation

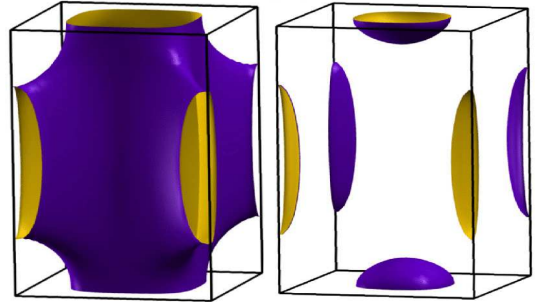


FIG. 5: Fermi surfaces of $x=0.20$ Sr hole doped NdNiO_2 , in the rigid band approximation, for case AFM0 (non-magnetic Ni) as defined in the main text. The region shown is the folded zone corresponding to AFM $4f$ alignment. Surfaces have been separated into left and right sub-panels for clarity. These surfaces can be compared with the bottom panel of Fig. 3 in the main text, which provides the surfaces in the virtual crystal approximation. The Γ -centered electron pocket has been emptied, while the k_z dispersion is increased substantially. (The undoped case is also given in the top panel of Fig. 3 in the main text.)

GGA+U electronic structure of ferromagnetic state

We provide here and below fatband plots indicating band character for all Ni $3d$ and Nd $5d$ orbitals, for both FM and AFM1 magnetic alignments (fully aligned moments; both Ni and Nd moments antialigned). The differences, also compared to the information in the main text for non-magnetic Ni, indicate how the various characters are shifted by relative magnetic alignment. Although ordering does not occur down to the lowest temperature measured, the differences give an indication of the effects of spin fluctuations. Some of the points to notice are included in the captions.

The spin-resolved fatband plots of separate Ni $3d$ and

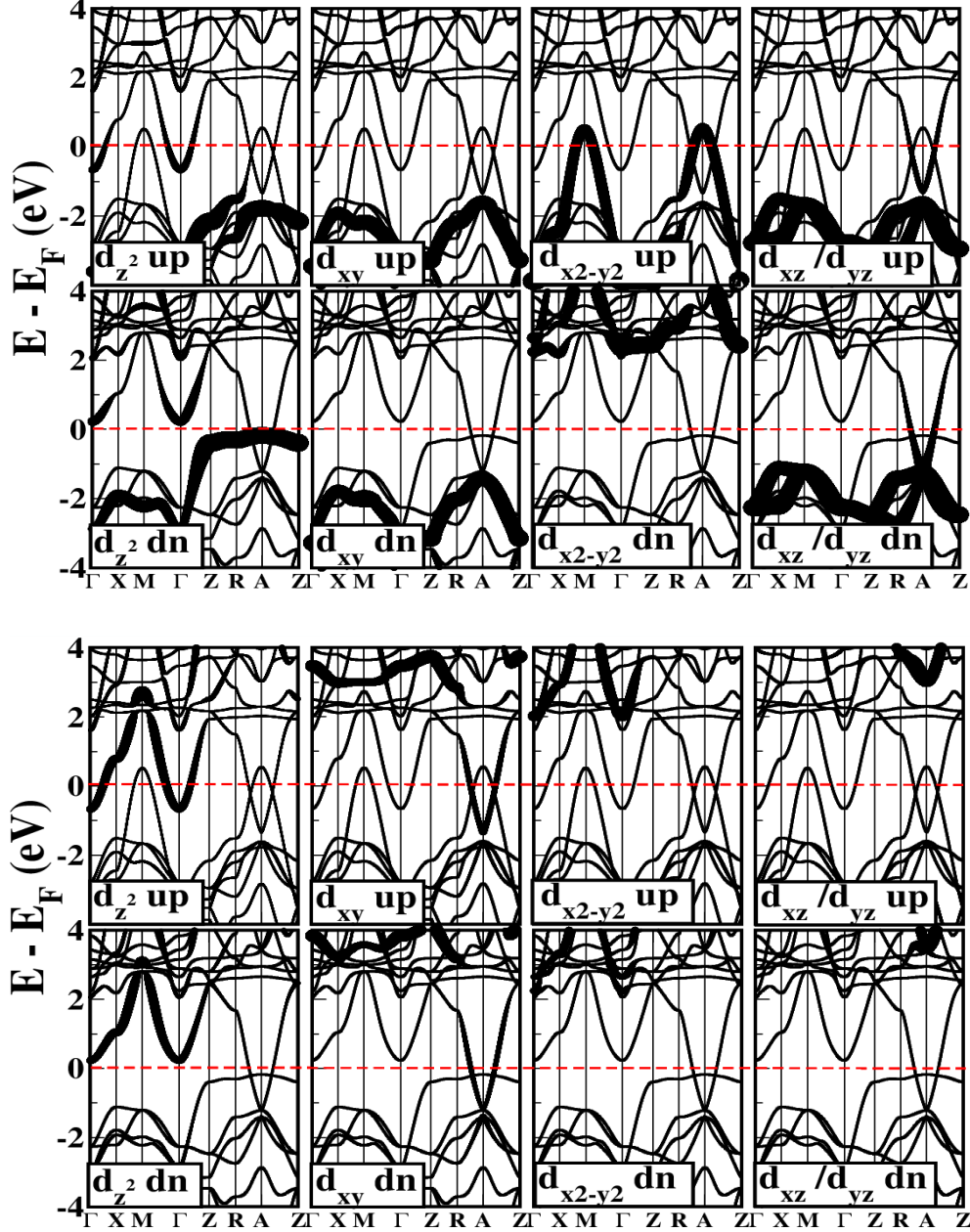


FIG. 6: Top: Fatband plots for all Ni $3d$ orbitals for FM alignment, with the GGA+U functional (see main text and section above for methods and values of interactions). Majority (up) bands are given in the upper panels, minority (down) in the lower panels. Note that there is some Ni d_{z^2} character for both spin directions in the Γ centered electron pocket. There is very strong Ni d_{z^2} character almost at E_F in the minority bands along the zone edge $Z - R - A - Z$.

Bottom: Fatband plots for all Nd $5d$ orbitals corresponding to those of Ni $3d$, above. Majority (up) bands are in the upper panels, minority (down) bands are in the lower panels. Strong Nd $5d$ character (d_{z^2}) is confined to the electron pockets Pk1 at Γ . There is lesser Nd contribution (d_{xy}) to the electron pocket Pk2 at A .

Nd $5d$ orbitals in the range of -4 eV to 4 eV for FM alignment of all moments are displayed in Fig. 6. Some aspects to note follow. The electron pocket band at the Γ point (fully spin polarized for this FM alignment) has strong Nd $5d_{z^2}$ character as noted by others, but it is mixed with significant Ni $3d_{z^2}$ character near the Γ point.

For the electron pocket at $A = (\pi, \pi, \pi)$ there is admixture of Ni $3d_{xz}/3d_{yz}$ character with the Nd $5d_{xy}$ orbitals. The hole bands at the M and A points have the primary $d_{x^2-y^2}$ character as occurs in cuprates.

Figure 7 displays the GGA+U orbital- and atom-projected densities of states (PDOSs) for FM alignment.

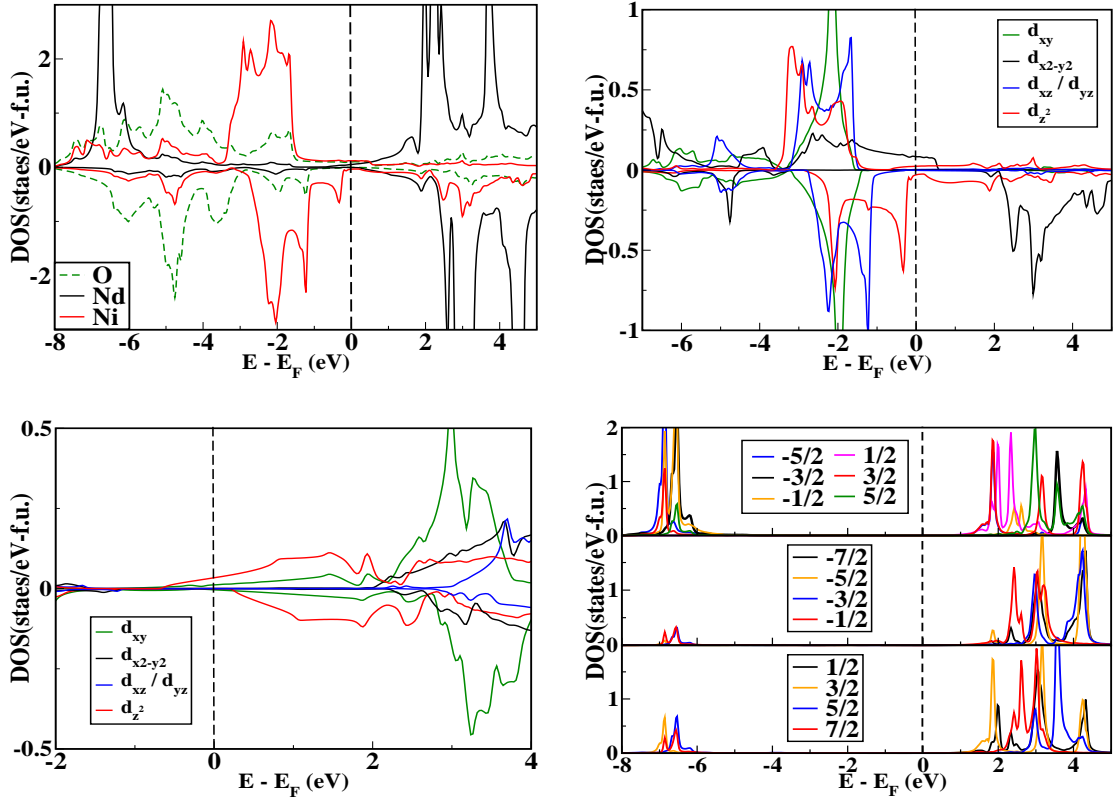


FIG. 7: FM projected densities of states (PDOSs) in GGA+U. Top left: atom PDOS. Top right: Ni 3d orbital PDOS. Bottom left: Nd 5d orbital PDOS. Bottom right: FM orbital-resolved DOSs of Nd 4f orbitals in the $|j, m_j\rangle$ basis, using GGA+U+SOC. The occupied orbitals are mostly $|5/2, -5/2\rangle$, $|5/2, -3/2\rangle$, and $|5/2, -1/2\rangle$ characters. Minor mixing with $|5/2, 5/2\rangle$, $|5/2, 3/2\rangle$ orbitals lead to an orbital moment of $-2.6 \mu_B$.

The Nd 4f-orbital resolved DOSs obtained from GGA+U+SOC are given in the bottom right panel of Fig. 7. The main effect of SOC is to produce, via introduced anticrossings, individual flat bands giving rise to separated DOS peaks for each orbital $|j, m_j\rangle$.

GGA+U electronic structures of antiferromagnetic states

To consider antiferromagnetic (AFM) states, a $\sqrt{2} \times \sqrt{2}$ supercell is necessary. As mentioned in the main text, we considered three AFM states and a fully aligned configuration:

- * AFM0: nonmagnetic Ni and AFM ordered Nd
- * AFM1: both AFM ordered Ni and Nd ions
- * AFM2: AFM ordered Ni and FM ordered Nd
- * FM: both sublattices completely aligned.

Here we provide additional information of AFM1 and AFM2, both of which have AFM Ni layers. For the AFM0 state, see the main text.

In GGA+U, similar to the FM cases, the magnitude of the local spin moments are $3 \mu_B$ for Nd and around $1.2 \mu_B$ for Ni. In AFM2, the FM ordered Nd moment induces a very small difference between up and down Ni moments of $0.03 \mu_B$, indicating the weakness but non-

vanishing of the magnetic Nd-Ni coupling as noted by others.

Figure 8 shows the band structures along lines in the AFM zone and atom-PDOSs of AFM1 and AFM2. (In the band structure plots, the *prime* symbol is omitted for simplicity.) Both band structures are characterized by a near gap as a cuprate would display, except for a band dispersing upward from $Z' - R'$ and downward from $a' - Z'$ along the $k_z = \pi$ plane. No such dispersion is observed on the $k_z = 0$ plane $\Gamma - X' - M' - \Gamma$. The Fermi level is fixed not by half-filling of this band but by the lower conduction band, which is flat along $Z' - R' - A' - Z'$. The dispersion band is of ambiguous mixed character while the flat band has very strong Ni d_{z^2} character.

In GGA, a magnetic Ni ion leads to a 120 meV energy gain compared to non-magnetic Ni. This exaggerated tendency toward magnetic ordering and the magnitude of the magnetic moment is a known deficiency of (semi)local density functional methods, with much of the problem attributed to the lack of effects of spin fluctuations in the functional.

The energies of AFM1, AFM2, and FM, obtained with the same functional, can be compared. The energy of AFM2 (FM Nd) is slightly lower than that of AFM1 (AFM Nd), by 7 meV for $U=0$ and by only 1 meV (at

the edge of computational precision) with $U=5$ eV on Ni, reflecting a slight tendency toward FM ordering of the $4f$ moments. The energy difference between FM and AFM2 provides the difference between AFM and FM Ni moments; AFM alignment is favored by 116 (25) meV/Ni in GGA(+U). This energy difference contains information about Ni-Ni in-plane exchange coupling, and would give a value of the nearest neighbor coupling if all others were negligible. Liu *et al.* have derived values of coupling for a few neighbors, concluding that the values depend strongly on the value of U^{Ni} that are used.[18]

Results of AFM1 and AFM2 show similarity as expected, with differences in the band structures appearing as small spin-splitting of bands, most evident in the Nd $5d$ electron-pocket band at Γ . Curiously, this band becomes incredibly flat along the zone-top lines $Z - R - A - Z$, pinning the Fermi level. The flatness

leads to a sharp peak at the Fermi level with the associated tendency toward instabilities of various kinds, and might contribute to the lack of such ordering.

We display the simpler band structure of AFM1, with the fatband plots of Ni $3d$ and Nd $5d$ presented separately in Figs. 9 and 10, respectively. The flat band at the Fermi level is seen to be very strongly Ni d_{z^2} in character. The corresponding orbital-projected DOSs are given in Fig. 11, where the Ni d_{z^2} peak is very prominent at the Fermi level – purely of a single character.

We also considered the effects of SOC in the GGA+U+SOC to analyze the Nd $4f$ configuration, leading to the Nd orbital moment of $-4.45 \mu_B$. Figure 12 shows the PDOS of Nd $4f$ orbitals in the $|j, m_j\rangle$ basis. Figure 13 shows the band structure and atom-projected DOS, when applying U and J only to the Nd $4f$ orbitals in the AFM1 alignment.

[1] J. P. Perdew, K. Burke, and M. Ernzerhof, Phys. Rev. Lett. **77**, 3865 (1996).

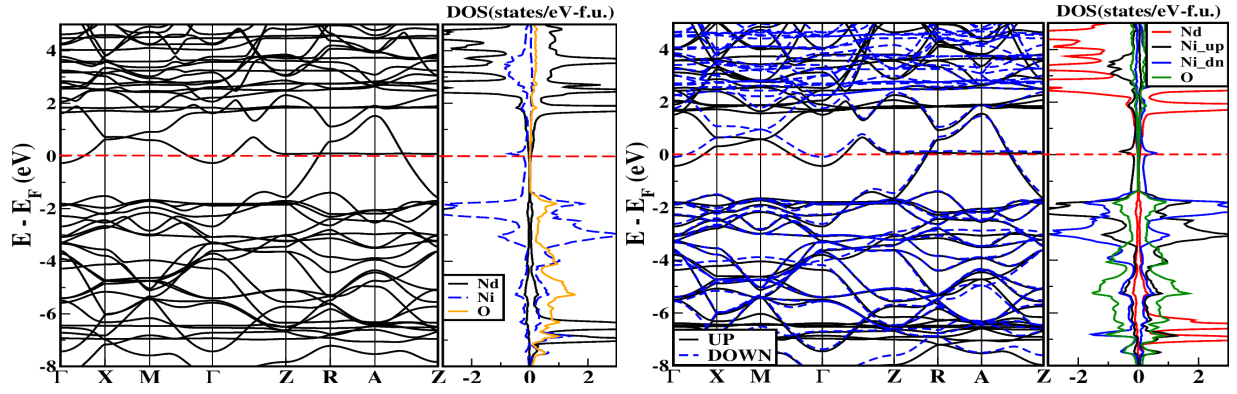


FIG. 8: GGA+U band structures and atom-projected DOSs of (left) AFM1 and (right) AFM2. In the AFM2 state, a small spin-imbalance in the antiferromagnetic ordered Ni ions is induced by the FM ordered Nd ions (see the region near E_F). Note that in both cases a flat band along $Z - R - A - Z$ pins the Fermi level.

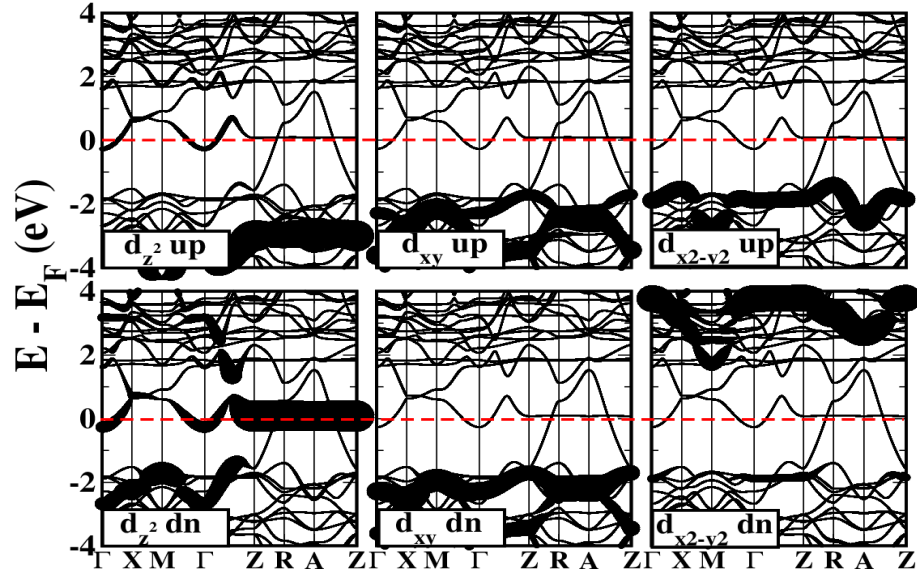


FIG. 9: AFM1 full fatband plots of Ni 3d orbitals in GGA+U. The fully occupied d_{xz}/d_{yz} orbitals are not shown here.

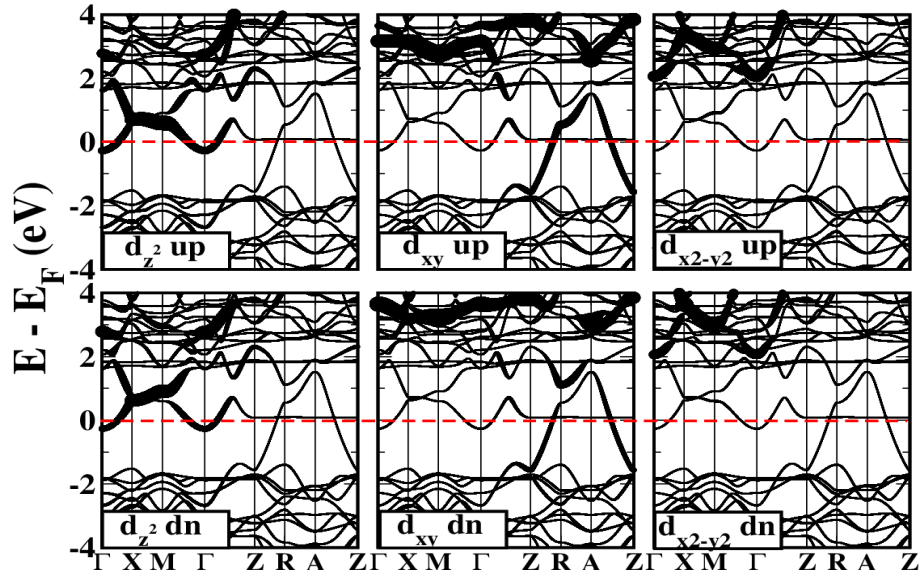


FIG. 10: AFM1 full fatband plots of Nd 5d orbitals in GGA+U. The fully unfilled d_{xz}/d_{yz} orbitals are not shown here.

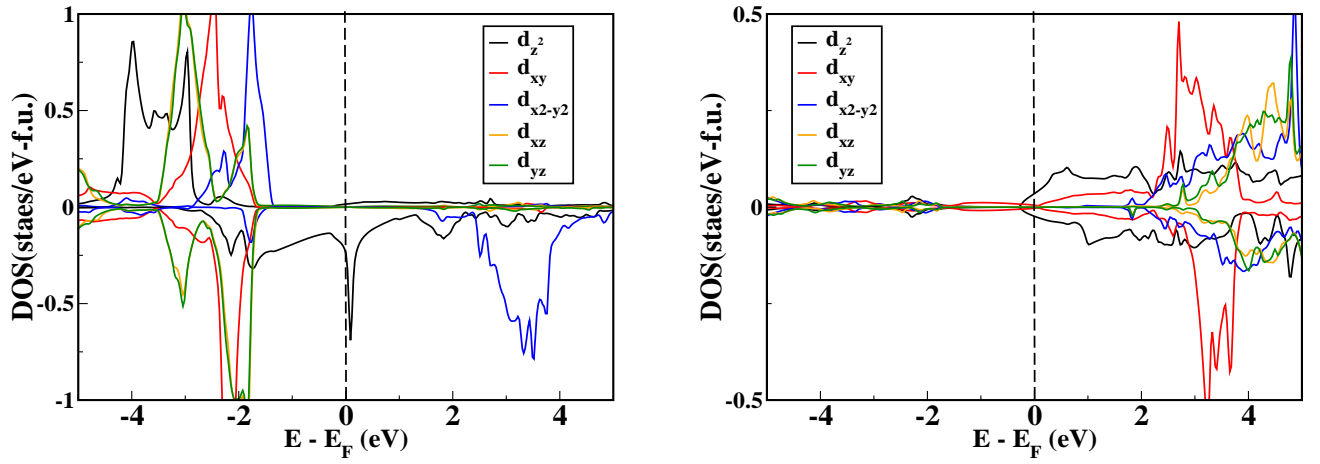


FIG. 11: AFM1 orbital-projected densities of states of (left) Ni 3d and (right) Nd 5d orbitals in GGA+U.

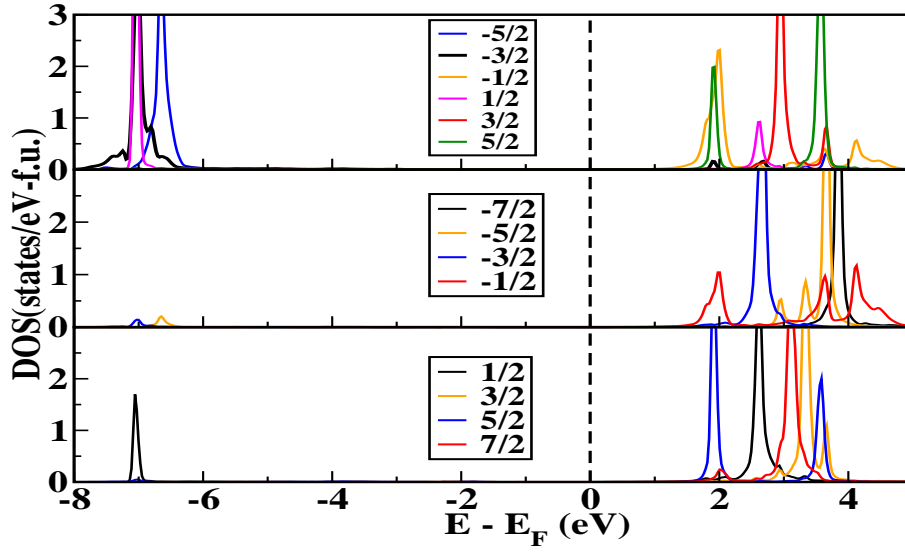


FIG. 12: AFM1 orbital-resolved DOSs of Nd 4f orbitals in the $|j, m_j\rangle$ basis, using the GGA+U+SOC. The occupied orbitals have mostly $|5/2, -5/2\rangle$, $|5/2, -3/2\rangle$, and $|5/2, +1/2\rangle$ character, leading to the 4f orbital moment of $-4.45 \mu_B$. Other configurations of similar energy might be obtained as self-consistent solutions, in which case the orbital moment would differ.

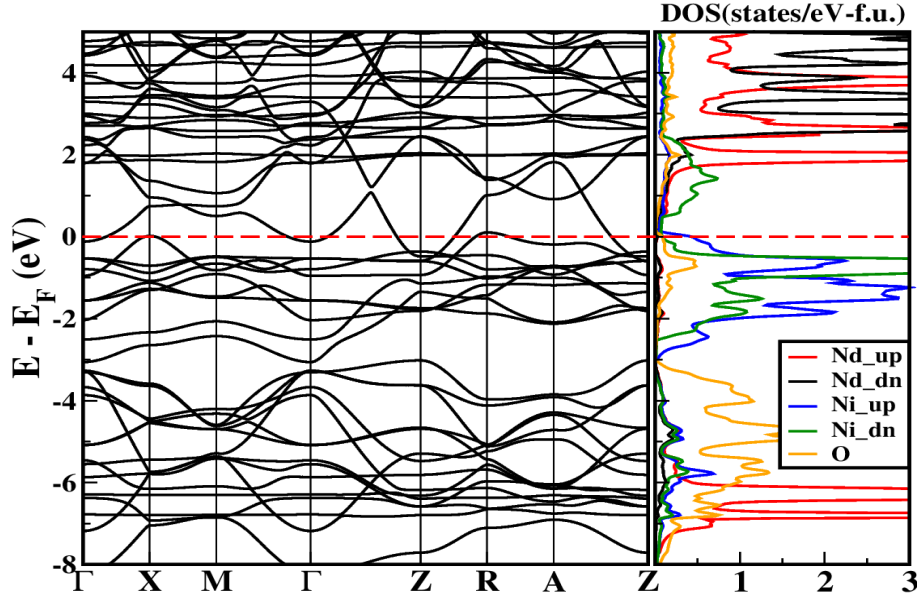


FIG. 13: AFM1 band structure and atom-projected DOSs in GGA+U, applying $U = 8$ eV and $J = 1$ eV only to the Nd 4f orbital. The magnitudes of the local spin moments are Nd $3 \mu_B$ and Ni $0.65 \mu_B$. Compared with that of applying U to both Ni and Nd orbitals (see Fig. 8), a clear distinction appears on the $k_z = \pi$ plane (along the Z-R-A-Z line), in addition to a few hole Fermi surface. In this case, the Ni $3d_{z^2}$ orbital, which is dispersionless in this plane, is fully occupied, and an electron band appears at the Z-point.